2011 American Control Conference
on O'Farrell Street, San Francisco, CA, USA
June 29 - July 01, 2011

Fractional Order Adaptive Feedforward Cancellation

Ying Luo§, YangQuan Chen‡ and YouGuo Pi£

Abstract— **In this paper, a fractional order adaptive feedforward cancellation (FO-AFC) scheme is proposed to cancel the periodic disturbance. This FO-AFC offers one more tuning knob – the fractional order, for the performance improvement of the periodic disturbance cancellation, according to the interests of the users. The equivalence of fractional order internal model principle (FO-IMP) scheme is derived for FO-AFC. So, the FO-IMP equivalence can be used to analyze the performance of the cancellation for the target periodic disturbance and the suppression for the harmonics and noise. Two FO-AFC cases, fractional order $\alpha \in (0,1)$ and $\alpha \in (1,2)$, are discussed for the performance analysis, respectively. FO-AFC with additional tuning knob $\alpha \in (0,2)$ has many advantages, and is much more flexible over the integer order adaptive feedforward cancellation (IO-AFC) with only $\alpha = 1$. Simulation results are presented to validate the performance analysis of FO-AFC comparing with IO-AFC.**

Index Terms— **Fractional order calculus, periodic disturbance, fractional order adaptive feedforward cancellation, fractional order internal model principle.**

I. INTRODUCTION

In practice, the periodic disturbances exist in variety of electromechanical systems. For example, the repeatable runout (RRO) problem in hard disk drive (HDD) digital servo systems is typically caused by the periodic disturbance which is one of the main contributors to track misregistration [1][2]; the cogging force in the permanent magnetic motors was defined as the position periodic disturbance in [3] and [4]. The challenges of compensating for periodic disturbances appear in various applications. Numerous control design methods have been developed specifically for eliminating periodic disturbances. Repetitive control [5] and disturbance observer (DOB) based control [6][7] have demonstrated effective compensation for repeatable disturbances. However, repetitive control tends to amplify nonrepeatable disturbances between the frequencies of the repeatable disturbances while DOB based control can alter the closed-loop properties of the system.

Another method of designing controllers to cancel periodic disturbances is the Internal Model Principle (IMP) proposed by Francis and Wonham [8] in 1976, which showed that a suitably reduplicated model of the disturbance dynamic structure should be included in feedback loop for perfect disturbance cancellation.

Adaptive feedforward cancellation (AFC) is also a well established method to reject sinusoidal disturbance with a known period but with unknown amplitude and unknown phase [9], which is essentially a special case of more general narrow-band disturbance rejection methods [10]. The adaptive algorithm can be used to estimate the unknown amplitude and unknown phase of the periodic disturbance. So, the negative of the disturbance value can be added to the input of the plant, then the periodic disturbance can be cancelled simply. AFC has been used in hard disk drive industry as a standard technique to cancel the once per revolution (OPR) disturbance due to the spindle motor runout [5]. AFC technique has also been extended to the case when the period is constant but unknown [11][12] and to the case when the disturbance is sinusoidal with respect to the state rather than the time [13].

In [9], the authors observed that the AFC algorithm was not only successful in eliminating the first harmonic but also in reducing the third harmonic of the periodic disturbance. The AFC algorithm designed to cancel the first harmonic may be capable of reducing the amplitude of the third harmonic as well. The generation of harmonics in the AFC algorithm was found to be due to the time-variation of the adaptive parameters and was explained using modulation arguments from standard signals and systems theory. The results of the analysis originate from the fact that the AFC algorithm is equivalent in some sense to an IMP algorithm.

In recent years, the applications of fractional calculus have been attracting more and more researchers in science and engineering [14][15][16][17][18][19][20][21][22]. In this paper, a fractional order adaptive feedforward cancellation (FO-AFC) scheme is proposed to cancel the periodic disturbance, which offers one more tuning knob, the fractional order, for the performance improvement of the periodic disturbance cancellation according to the interests of the users. The equivalence of fractional order internal model principle (FO-IMP) scheme is derived for FO-AFC. Thus, the FO-IMP equivalence can be used to analyze the performance of the cancellation for the target periodic disturbance and the suppression for the harmonics and noise, by the Bode plots of the sensitivity functions of the closed-loop system. Two FO-AFC cases, fractional order $\alpha \in (0,1)$ and $\alpha \in (1,2)$, are proposed for the performance analysis, respectively. First, FO-AFC with $\alpha \in (0,1)$ has narrower slot around the frequency of the target periodic disturbance over IO-AFC in the Bode plots of the sensitivity functions, which means FO-AFC with $\alpha \in (0,1)$ is more selective for the cancellation of the target periodic disturbance with the desired cancellation capability shown as the slot depth in the Bode plots. Meanwhile, the amplitude of FO-AFC with $\alpha \in (0,1)$ is much smaller over that of IO-AFC at higher frequency in the Bode plots of the sensitivity functions, which reveals that the suppression capability of FO-AFC with $\alpha \in (0,1)$ is stronger than that of IO-AFC for the high-order harmonics of the target periodic disturbance or the high frequency noise. Second, FO-AFC with $\alpha \in (1,2)$ has deeper slot at the frequency of the target periodic disturbance over IO-AFC, and the amplitude of FO-AFC with $\alpha \in (1,2)$ around the frequency of the target periodic disturbance is lower than that of IO-AFC, which indicates FO-AFC with $\alpha \in (1,2)$ is not so selective as IO-AFC for the cancellation of the target periodic disturbance, but the suppression performance of FO-AFC with $\alpha \in (1,2)$ is better than that of IO-AFC for the disturbances or noise around the frequency of the target periodic disturbance. Meanwhile, there is also a disadvantage for FO-AFC with $\alpha \in (1,2)$, the amplitudes of FO-AFC with $\alpha \in (1,2)$ is bigger than that of IO-AFC at a range of higher frequency in the Bode plots of the sensitivity functions, which means FO-AFC with $\alpha \in (1,2)$ may amplify the high-order harmonics of the target periodic disturbance or the high frequency noise comparing with IO-AFC. Anyhow, FO-AFC with additional tuning knob $\alpha \in (0,2)$ has advantages and is much more flexible over IO-AFC with only $\alpha = 1$ for the cancellation of the target periodic disturbance and the suppression of the harmonics or the noise. Simulation results are presented to validate the performance analysis of FO-AFC comparing with IO-AFC.

§Department of Automation Science and Engineering, South China University of Technology, Guangzhou, P. R. China; and with Department of Electrical and Computer Engineering, Utah State University, Logan, UT, USA;

‡Email: yqchen@ece.usu.edu, Department of Electrical and Computer Engineering, Utah State University, Logan, UT 84322, USA;

£Department of Automation Science and Engineering, South China University of Technology, Guangzhou, P. R. China.

The major contributions of this paper include: 1) a new fractional order adaptive feedforward cancellation scheme; 2) equivalence derivation of the fractional order internal model principle scheme; 3) analysis of the benefits and trade-offs of using the fractional order adaptive feedforward cancellation scheme with the additional tuning knob – fractional order $\alpha \in (0,1)$ and $\alpha \in (1,2)$; 4) Simulation illustration of the performance analysis of FO-AFC comparing with that of IO-AFC.

The remaining part of this paper is organized as follows. In Sec. II, the new fractional order feedforward cancellation scheme is proposed. In Sec. III, the equivalence of the fractional order internal model principle is deduced and in Sec. IV, the performance of FO-AFC is analyzed through the Bode plots of the sensitivity functions. Simulation illustration is presented in Sec. V. Finally, the conclusion is given in Sec. VII.

II. Fractional Order Adaptive Feedforward Cancellation

In this section, a fractional order adaptive feedforward cancellation scheme is proposed with an extra tuning knob – fractional order. Assuming that the disturbance is set as follows,

$$d(t) = A\sin(\omega_1 t + \phi) = a_1\cos(\omega_1 t) + b_1 \sin(\omega_1 t). \quad (1)$$

As shown in Fig.1, the control input of the plant is selected to be,

$$u(t) = \theta_1(t)\cos(\omega_1 t) + \theta_2(t)\sin(\omega_1 t), \quad (2)$$

and the plant output can be written as,

$$y(t) = Ł^{-1}[Ł((\theta_1(t) - \theta_1^*)\cos(\omega_1 t) + (\theta_2(t) - \theta_2^*)\sin(\omega_1 t))P(s)], \quad (3)$$

where, $Ł(\cdot)$ stands for the Laplace transform; θ_1^* and θ_2^* denote the nominal values of $\theta_1(t)$ and $\theta_2(t)$, respectively. So that, when

$$\theta_1^* = -a_1, \theta_2^* = -b_1,$$

and if the parameters $\theta_1(t)$ and $\theta_2(t)$ converge to the nominal values, the disturbance $d(t)$ can be exactly canceled.

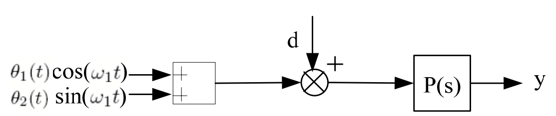

Fig. 1. Fractional order adaptive feedforward cancellation.

In this study the following Caputo definition is adopted for fractional derivative, which allows utilization of initial values of classical integer-order derivatives with known physical interpretations [23], [22],

$$ {}_0D_t^\alpha f(t) = \frac{\mathrm{d}^\alpha f(t)}{\mathrm{d}t^\alpha} = \frac{1}{\Gamma(\alpha - n)}\int_0^t \frac{f^{(n)}(\tau)}{(t-\tau)^{\alpha+1-n}}\mathrm{d}\tau, \quad (4)$$

where n is an integer satisfying $n-1 < \alpha \leq n$, α is the order of the fractional derivative, $f^{(n)}(\tau)$ is the $n-th$ derivative of $f(\tau)$, and $\Gamma(x)$ is the Gamma function with the definition below,

$$\Gamma(x) = \int_0^\infty t^{x-1}e^{-t}\mathrm{d}t.$$

From equations (2.242) and (2.248) in [23]

$$L\{{}_0D_t^{-p}f(t); s\} = s^{-p}F(s), \quad (5)$$

where $0 < p$.

$$L\{{}_0D_t^p f(t); s\} = s^p F(s) - \sum_{k=1}^{n-1} s^k[{}_0D_t^{p-k-1}f(t)]_{t=0}, \quad (6)$$

where $0 \leq n-1 \leq p < n$.

Then, a fractional order possible update law for the adaptive parameters is proposed as follows,

$$ {}_0D_t^\alpha \theta_1(t) = -gy(t)\cos(\omega_1 t), \quad (7)$$

$$ {}_0D_t^\alpha \theta_2(t) = -gy(t)\sin(\omega_1 t), \quad (8)$$

where the fractional order $\alpha \in (0,2)$, and $g > 0$ is an arbitrary parameter called the fractional order adaptation gain.

In (3.5) of [9], the traditional integrator was used for the adaptive law, namely, the integer order feedforward cancellation (IO-AFC) was applied with $\alpha = 1$ in (7) and (8). IO-AFC algorithm designed to cancel the first harmonic may be capable of reducing the amplitude of the third harmonic as well. The generation of harmonics in IO-AFC algorithm was found to be due to the time-variation of the adaptive parameters and was explained using modulation arguments from standard signals and systems theory in [9].

In order to compare the proposed FO-AFC with IO-AFC in [9] fairly, the same plant and disturbance in [9] were used in this FO-AFC scheme test as shown below,

$$P(s) = \frac{s+2}{(s+1)(s+3)}, \quad (9)$$

$$d(t) = \sin(0.1t) - 0.2\sin(0.3t), \quad (10)$$

where all initial conditions are zero, and the adaptive gain is set as $g = 1$. The disturbance has a fundamental component at $0.1\ rad/s$ and a third harmonic at $0.3\ rad/s$.

Fig. 2(a) shows the response $y(t)$ of the system without any compensation. The first and third harmonics are clearly visible. Fig. 2(b) is the response $y(t)$ of the system for $\theta_1(t)$ and $\theta_2(t)$ frozen to $\theta_1^*(t)$ and $\theta_2^*(t)$, respectively. The first harmonic is canceled exactly and the third harmonic is unchanged. In Fig. 3, the blue line stands for the response $y(t)$ using IO-AFC, just the same as Fig. 5 in [9], not only is the first harmonic eliminated, but also is the third harmonic significantly reduced; and the red line shows the response $y(t)$ using FO-AFC with $\alpha = 1.5$ in (7) and (8). It is obvious that, the magnitude of the third harmonic using FO-AFC with $\alpha = 1.5$ is much smaller than that using IO-AFC, which can also be seen clearly from the FFT spectrum w. r. t. the frequency in Fig. 4.

The parameter values of $\theta_1(t)$ and $\theta_2(t)$ is shown in Fig. 5. $\theta_1(t)$ and $\theta_2(t)$ should converge to the nominal values $\theta_1^*(t) = -a_1 = 0$ and $\theta_2^*(t) = -b_1 = -1$, respectively. If the disturbance is only the first harmonic, the parameters indeed converge toward these nominal values. But, because of the third harmonic, there is substantial fluctuation of the parameters in the steady state, and the variations can be recognized as second and fourth harmonics of the fundamental frequency. The solid and dashed blue lines in Fig. 5 stand for the parameter values of $\theta_1(t)$ and $\theta_2(t)$ using IO-AFC method; the solid and dashed red lines show the parameter values of $\theta_1(t)$ and $\theta_2(t)$ using the proposed FO-AFC scheme with $\alpha = 1.5$. We can see that, the fluctuation amplitude of $\theta_1(t)$ and $\theta_2(t)$ using the $\alpha = 1.5$ FO-AFC is much bigger than that using IO-AFC.

The time-variation of the parameters $\theta_1(t)$ and $\theta_2(t)$ generates a third harmonic that is not present in the ideal case. This component of the input reduces the amplitude of the third harmonic observed at the output of the plant. This leads to the observation that the adaptive scheme with parameters $\theta_1(t)$ and $\theta_2(t)$ performs better in the presence of higher-order harmonics than the scheme with the fixed nominal parameters $\theta_1^*(t)$ and $\theta_2^*(t)$. So, with bigger fluctuation amplitude of $\theta_1(t)$ and $\theta_2(t)$, the $\alpha = 1.5$ FO-AFC scheme can reduce the amplitude of the third harmonic more effectively than IO-AFC scheme, which can be seen in Fig 3 and Fig. 4.

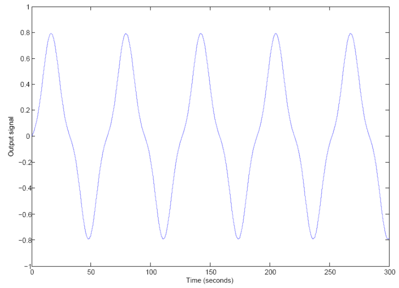

(a) Without compensation

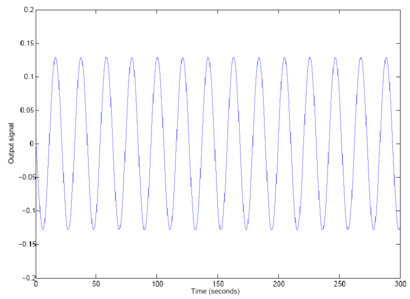

(b) With fixed nominal compensation

Fig. 2. Output without compensation / with fixed nominal compensation.

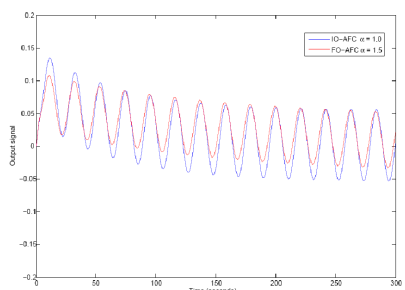

Fig. 3. Output with IO-AFC and α=1.5 FO-AFC

III. Equivalence Between Fractional Order Internal Model Principle and Fractional Order Adaptive Feedforward Cancellation

A. Single-Frequency Disturbance Cancellation

For the fractional order adaptive feedforward cancellation for a single-frequency disturbance, the input and disturbance signals are shown as (1) and (2), respectively. The fractional order adaptive updating law is presented as (7) and (8).

Since, one has,

$$e^{j\omega_1 t} = \cos\omega_1 t + j\sin\omega_1 t,$$

and

$$e^{-j\omega_1 t} = \cos\omega_1 t - j\sin\omega_1 t.$$

So, from (1), we can obtain,

$$\begin{aligned} u(t) &= \theta_1(t)(e^{j\omega_1 t} - j\sin(\omega_1 t)) \\ &\quad + \theta_2(t)(e^{j\omega_1 t} - \cos(\omega_1 t))(-j), \quad (11) \\ u(t) &= \theta_1(t)(e^{-j\omega_1 t} + j\sin(\omega_1 t)) \\ &\quad + \theta_2(t)(e^{-j\omega_1 t} - \cos(\omega_1 t))j. \quad (12) \end{aligned}$$

Then add (11) and (12), we can get,

$$u(t) = \frac{\theta_1(t)}{2}(e^{j\omega_1 t} + e^{-j\omega_1 t}) + \frac{j\theta_2(t)}{2}(e^{-j\omega_1 t} - e^{j\omega_1 t}). \quad (13)$$

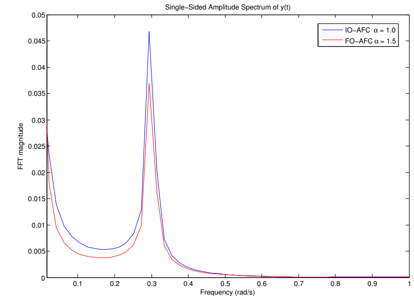

Fig. 4. FFT spectrum with IO-AFC and α=1.5 FO-AFC

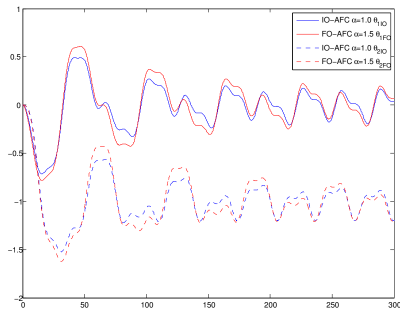

Fig. 5. Adaptive parameter values of $\theta_1(t)$ and $\theta_2(t)$ with IO-AFC and α=1.5 FO-AFC.

In the same way, from (7) and (8), yield,

$$ {}_0D_t^\alpha \theta_1(t) = -\frac{g}{2} y(t)(e^{j\omega_1 t} + e^{-j\omega_1 t}), \quad (14)$$

$$ {}_0D_t^\alpha \theta_2(t) = -\frac{jg}{2} y(t)(e^{-j\omega_1 t} - e^{j\omega_1 t}). \quad (15)$$

$U(s)$ and $Y(s)$ are the Laplace transforms of the input $r(t)$ and output $y(t)$, respectively. Similarly, mark $\Theta_1(s)$ and $\Theta_2(s)$ as the Laplace transforms of the $\theta_1(t)$ and $\theta_2(t)$ with initial condition, $\theta_1(t)|_{t=0} = \theta_2(t)|_{t=0} = 0$.

From (14) and (15) we can derive that [23] ,

$$\begin{aligned} \Theta_1(s) &= -\frac{g}{2s^\alpha}(Y(s+j\omega_1) + Y(s-j\omega_1)), \quad (16) \\ \Theta_2(s) &= -\frac{jg}{2s^\alpha}(Y(s-j\omega_1) - Y(s+j\omega_1)). \quad (17) \end{aligned}$$

Then, from (13), (16) and (17) we can get,

$$\begin{aligned} U(s) &= \frac{1}{2}(\Theta_1(s-j\omega_1) + \Theta_1(s+j\omega_1)) \\ &\quad + \frac{j}{2}(\Theta_2(s-j\omega_1) - \Theta_2(s+j\omega_1)) \\ &= -\frac{g}{2}\left(\frac{1}{(s+j\omega_1)^\alpha} + \frac{1}{(s-j\omega_1)^\alpha}\right)Y(s) \\ &= -gC_{IMP}(s)Y(s), \quad (18) \end{aligned}$$

where $C_{IMP}(s) = \frac{(s-j\omega_1)^\alpha + (s+j\omega_1)^\alpha}{2(s^2+\omega_1^2)^\alpha}$.

So, the fractional order adaptive feedforward cancellation scheme in Fig. 1 with adaptive law (7) and (8) can be equivalent to the

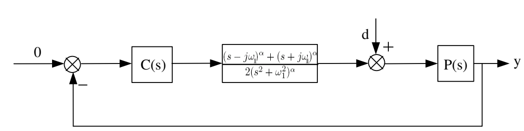

Fig. 6. Fractional order internal model principle equivalence of the fractional order adaptive feedforward cancellatio.

fractional order internal model principle scheme in Fig. 6 with $C(s) = g$. Actually, the controller $C(s)$ is not limited to be equal to g. For instance, let Y_c be a signal after a block $F(s)$, e.g., a filter, namely, $Y_c(s) = F(s)Y(s)$, and replace $Y(s)$ by $Y_c(s)$ in (7) and (8), then, FO-AFC scheme is equal to the FO-IMP scheme with $C(s) = gF(s)$. This modification can also be used to filter the signal u in (2) before it is applied to the plant.

B. Generalization to Multi-Frequency Disturbance Cancellation

This equivalence between FO-AFC and FO-IMP can be easily extended to the case when multiple frequency components are cancelled. For example, if u is replaced by,

$$\begin{aligned} u(t) &= \theta_1(t)\cos(\omega_1 t) + \theta_2(t)\sin(\omega_1 t) \\ &\quad +\theta_3(t)\cos(\omega_2 t) + \theta_4(t)\sin(\omega_2 t), \end{aligned} \tag{19}$$

where θ_1, θ_2 are updated by,

$$\begin{aligned} {}_0D_t^{\alpha}\theta_1(t) &= -g_1 y(t)\cos(\omega_1 t), \\ {}_0D_t^{\alpha}\theta_2(t) &= -g_1 y(t)\sin(\omega_1 t), \\ {}_0D_t^{\alpha}\theta_3(t) &= -g_2 y(t)\cos(\omega_2 t), \\ {}_0D_t^{\alpha}\theta_4(t) &= -g_2 y(t)\sin(\omega_2 t), \end{aligned}$$

then, FO-AFC system is equivalent to a FO-IMP control system with,

$$\begin{aligned} \frac{U(s)}{Y(s)} &= -g_1\frac{(s-j\omega_1)^{\alpha}+(s+j\omega_1)^{\alpha}}{2(s^2+\omega_1^2)^{\alpha}} \\ &\quad -g_2\frac{(s-j\omega_2)^{\alpha}+(s+j\omega_2)^{\alpha}}{2(s^2+\omega_2^2)^{\alpha}}. \end{aligned}$$

IV. Frequency-domain analysis of FO-AFC performance for the periodic disturbance

As introduced in Sec. III, FO-AFC scheme proposed can be equivalent to the FO-IMP scheme in Fig. 6 with $C(s) = g$. Thus, FO-AFC performance of the the cancellation of the target periodic disturbance and the suppression of the harmonics and noise can be analyzed in frequency-domain using the FO-IMP equivalence.

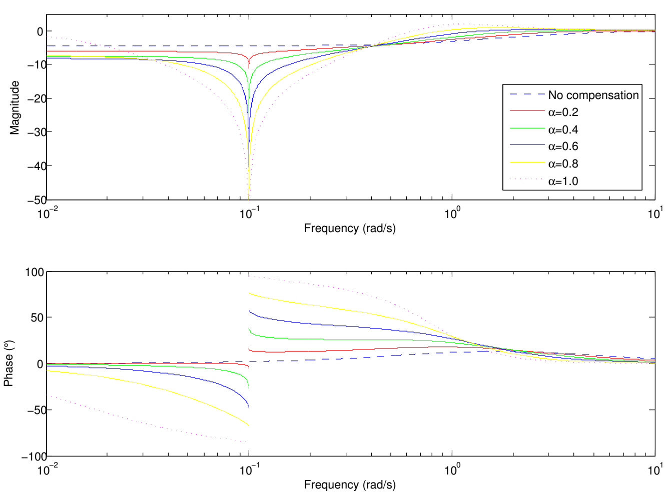

Fig. 7. Bode plots of the sensitivity function with $\omega_1 = 0.1$ and $\alpha \in (0, 1]$.

The sensitivity function of the system with FO-IMP in Fig. 6 is,

$$G_s(s) = \frac{1}{1 + C(s)C_{IMP}(s)P(s)}, \tag{20}$$

where $C_{IMP}(s) = \frac{(s-j\omega_1)^{\alpha}+(s+j\omega_1)^{\alpha}}{2(s^2+\omega_1^2)^{\alpha}}$. Since the FO-IMP equivalence is used for the analysis of FO-AFC scheme, the stability/instability boundary of the adaptive system can be predicted, according to the Lyapunov theory [24], Nyquist criterion [9], or the averaging analysis [25]. It can be seen that, the absolute value and the sign of the adaptive gain g are constrained for the stability of the adaptive system [25]. Therefore, for the fair comparison between the integer order AFC and the proposed FO-AFC, the same adaptive gain value is used for both schemes, e.g., $g = 1$. Then, the disturbance rejection performance using FO-AFC can be discussed and compared with that using traditional AFC scheme.

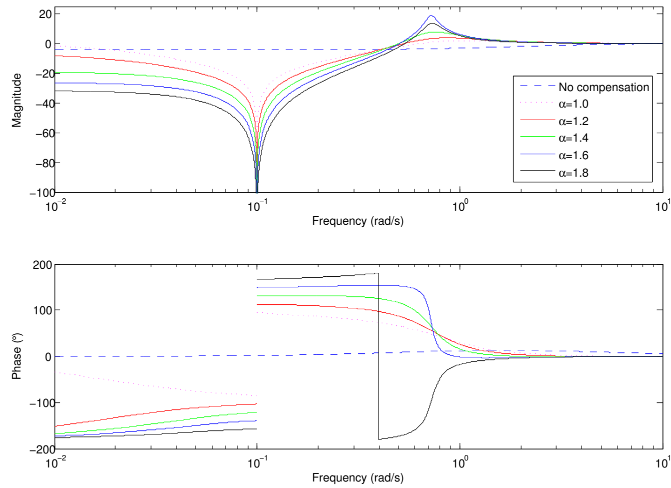

Fig. 8. Bode plots of the sensitivity function with $\omega_1 = 0.1$ and $\alpha \in [1, 2)$.

Following the plant (9) in Sec. II which is from [9], the sensitivity function of $G_s(s)$ can be derived as,

$$G_s(s) = \frac{2(s^2+\omega_1^2)^{\alpha}(s+1)(s+3)}{D(s)}, \tag{21}$$

where

$$\begin{aligned} D(s) &= 2(s^2+\omega_1^2)^{\alpha}(s+1)(s+3) \\ &\quad +g(s+2)[(s+j\omega_1)^{\alpha}+(s-j\omega_1)^{\alpha}]. \end{aligned} \tag{22}$$

Thus, the Bode diagram of $G_s(s)$ can be plotted in Fig. 7 and Fig. 8 with $\alpha \in (0, 2)$ and ω_1=0.1 rad/s.

From Fig. 7, it can be seen that, around the disturbance frequency ω_1=0.1 rad/s, the magnitudes of the sensitivity function with AFC compensation are much smaller than that without compensation presented by the dashed blue line. FO-AFC with $\alpha \in (0, 1)$ have narrower and shallower slot around the frequency ω_1=0.1 rad/s over IO-AFC, which means FO-AFC with $\alpha \in (0, 1)$ can also cancel the disturbance at the frequency ω_1=0.1 rad/s, and FO-AFC with $\alpha \in (0, 1)$ are more selective than IO-AFC for the cancellation of the target periodic disturbance with the desired cancellation capability shown as the slot depth in Fig. 7. Meanwhile, the magnitudes around ω_1=0.1 rad/s from 0.02 rad/s to 0.5 rad/s using FO-AFC with $\alpha \in (0, 1)$ are bigger than that using IO-AFC. But after 0.5 rad/s and before 0.02 rad/s, the magnitude with IO-AFC is bigger than that using FO-AFC with $\alpha \in (0, 1)$, which means FO-AFC with $\alpha \in (0, 1)$ have better effect of suppressing the higher-order harmonic disturbance or high frequency noise after 0.5 rad/s and before 0.02 rad/s; however, from 0.02 rad/s to 0.5 rad/s, the disturbance or noise suppression effect using FO-AFC with $\alpha \in (0, 1)$ is not as good as that using IO-AFC.

In Fig. 8, using FO-AFC with $\alpha \in (1, 2)$, we can see that, the magnitudes of the sensitivity function with AFC compensation are also much smaller than that without compensation, FO-AFC with $\alpha \in (1, 2)$ have deeper and wider slots around the frequency

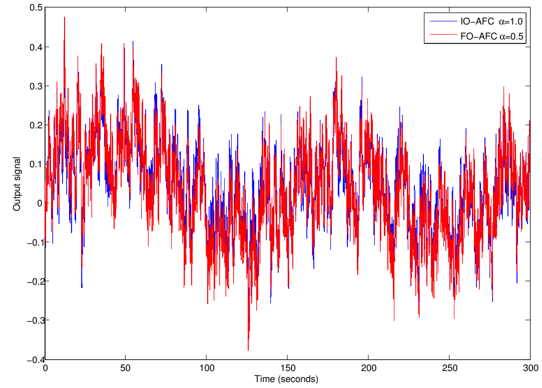

Fig. 9. Output signals with IO-AFC and FO-AFC of $\alpha = 0.5$.

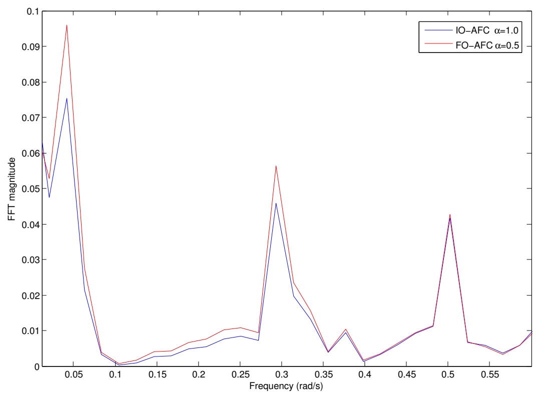

Fig. 10. FFT spectrum of the outputs with IO-AFC and FO-AFC of $\alpha = 0.5$ ($\omega \in [0, 0.6]$ rad/s).

ω_1=0.1 rad/s over IO-AFC, which means the disturbance at the frequency ω_1=0.1 rad/s can also be cancelled by the AFC with $\alpha \in [1, 2)$, and FO-AFC with $\alpha \in (1, 2)$ are not so selective as IO-AFC for the cancellation of the target periodic disturbance. At the same time, before 0.6 rad/s, the magnitudes with FO-AFC of $\alpha \in (1, 2)$ are smaller than that with IO-AFC. So, the disturbance or noise before 0.6 rad/s can be suppressed more effectively by FO-AFC of $\alpha \in (1, 2)$ than IO-AFC. However, there is also a trade-off, after the frequency 0.6 rad/s, the disturbance harmonics or noise should be amplified by FO-AFC with $\alpha \in (1, 2)$ comparing with using IO-AFC.

To sum up, FO-AFC with additional tuning knob $\alpha \in (0, 2)$ has advantages and is more flexible over IO-AFC with only $\alpha = 1$ for the cancellation of the target periodic disturbance and the suppression of the harmonics or the noise.

V. Simulation Illustration

In order to test the frequency-domain analysis results of disturbance cancellation performance of FO-AFC scheme, the simulation illustration is presented in this section. In the simulation, the system $P(s)$ as (9) is also used for the fair comparison, and the disturbance is designed as,

$$\begin{aligned} d(t) \;\; &= \;\; 0.5\sin(0.05t) + \sin(0.1t) - 0.2\sin(0.3t) \\ & \quad\; -0.1\sin(0.5t) + N(t), \end{aligned} \tag{23}$$

which contain the disturbance components in (10), where $N(t)$ is the white noise. In the control law (2), ω_1 is also chosen as 0.1 rad/s.

For FO-AFC with $\alpha \in (0, 1)$, we choose $\alpha = 0.5$ to test the performance and compare with IO-AFC, as shown in Figs. 9, 10 and 11. Fig. 9 is the output comparison of FO-AFC with $\alpha = 0.5$ and IO-AFC, where it is not easy to distinguish the performances of two methods because of the white noise. So, the FFT plots are presented in Fig. 10 and Fig. 11. In Fig. 10, it is obvious that, the disturbance at the frequency $\omega_1 = 0.1$ rad/s is almost canceled completely by not only IO-AFC but also FO-AFC of $\alpha = 0.5$. The disturbance magnitudes at the frequencies $\omega = 0.05$ rad/s, $\omega = 0.3$ rad/s and $\omega = 0.5$ rad/s using FO-AFC with $\alpha = 0.5$ are higher than that using IO-AFC, which is corresponded to the Bode plot feature in the frequency range $(0.02, 0.5)$ rad/s in Fig. 7. Meanwhile, the disturbance magnitude at the higher frequency range after 0.5 rad/s using FO-AFC with $\alpha = 0.5$ is lower than that using IO-AFC method, which can be seen in Fig. 11.

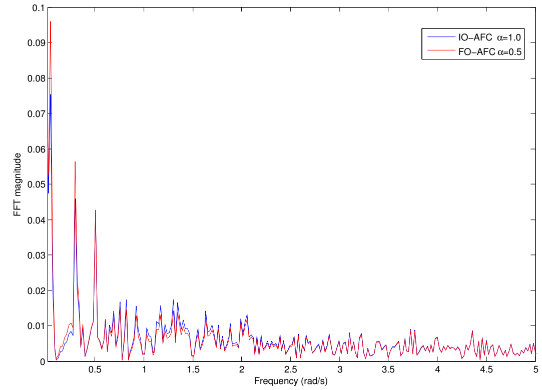

Fig. 11. FFT spectrum of the outputs with IO-AFC and FO-AFC of $\alpha = 0.5$ ($\omega \in [0, 5]$ rad/s).

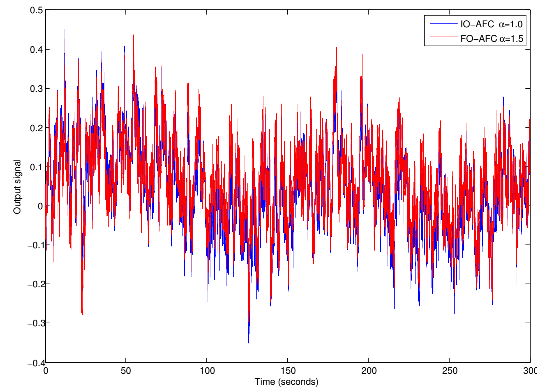

Fig. 12. Output signals with IO-AFC and FO-AFC of $\alpha = 1.5$.

As far as FO-AFC of $\alpha \in (1, 2)$ is considered, we choose $\alpha = 1.5$ to test the performance and compare with IO-AFC, which can be seen in Figs. 12, 13 and 14. The output comparison of FO-AFC with $\alpha = 1.5$ and IO-AFC is shown in Fig. 12, and the FFT plots are presented in Fig. 13 and Fig. 14. In Fig. 13, it can be seen that, the disturbance at the frequency $\omega_1 = 0.1$ is almost canceled completely by both IO-AFC and FO-AFC of $\alpha = 1.5$. The disturbance magnitudes at the frequencies $\omega = 0.05$, $\omega = 0.3$ and $\omega = 0.5$ using FO-AFC of $\alpha = 1.5$ are lower than that using IO-AFC, which is corresponded to the Bode plot feature in the frequency range $\omega < 0.6$ rad/s in Fig. 7. This result is consistent with Fig. 3 and Fig. 4 of the simpler disturbance example in Sec. II. Meanwhile, the disturbance magnitudes at the higher frequency after 0.6 rad/s using FO-AFC of $\alpha = 1.5$ is amplified comparing with that using IO-AFC, which can be seen in Fig. 14.

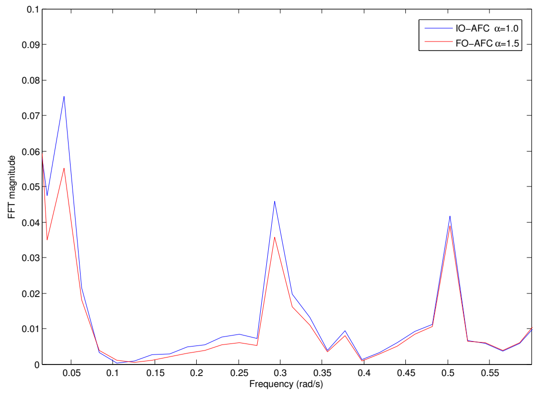

Fig. 13. FFT spectrum of the outputs with IO-AFC and FO-AFC of $\alpha = 1.5$ ($\omega \in [0, 0.6]$ rad/s).

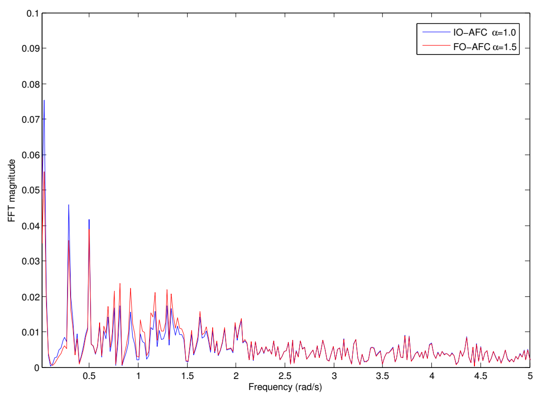

Fig. 14. FFT spectrum of the outputs with IO-AFC and FO-AFC of $\alpha = 1.5$ ($\omega \in [0, 5]$ rad/s).

VI. Experiment Validation

Omitted due to space limit.

VII. Conclusion

In this paper, a FO-AFC scheme is proposed to cancel the periodic disturbance. This FO-AFC offers one more tuning knob, the fractional order, for the performance improvement of the periodic disturbance cancellation according to the interests of the users. The equivalence of the FO-IMP scheme is derived for FO-AFC. Thus, the FO-IMP equivalence can be used to analyze the performance of the cancellation for the target periodic disturbance and the suppression for the harmonics and noise, by the Bode plots of the sensitivity functions of the closed-loop system. Two FO-AFC cases, fractional order $\alpha \in (0, 1)$ and $\alpha \in (1, 2)$, are proposed for the performance analysis, respectively. FO-AFC with additional tuning knob $\alpha \in (0, 2)$ has advantages and is much more flexible over IO-AFC for the cancellation of the target periodic disturbance and the suppression of the harmonics or the noise. Simulation results are presented to validate the performance analysis of FO-AFC comparing with IO-AFC.

References

[1] Chang Duan, Guoxiao Guo, Chunling Du, and Tow Chong Chong, "Robust compensation of periodic disturbances by multirate control," *IEEE Transactions on Magnetics*, vol. 44, no. 3, pp. 413–418, 2008.

[2] M.R. Graham and R.A. de Callafon, "An iterative learning design for repeatable runout cancellation in disk drives," *IEEE Transactions on Control Systems Technology*, vol. 14, no. 3, pp. 474–482, 2006.

[3] Ying Luo, YangQuan Chen, and YouGuo Pi, "Authentic simulation studies of periodic adaptive learning compensation of cogging effect in PMSM position servo system," in *Proceedings of the Chinese Conference on Decision and Control (CCDC08)*, Yantai, Shandong, China, 2-4 July 2008, pp. 4760–4765.

[4] Hyo-Sung Ahn, YangQuan Chen, and Huifang Dou, "State-periodic adaptive compensation of cogging and coulomb friction in permanent-magnet linear motors," *IEEE Transactions on Magnetics*, vol. 41, no. 1, pp. 90–98, 2005.

[5] Alexei Sacks, Marc Bodson, and William Messner, "Advanced methods for repeatable runout compensation," *IEEE Trans. on Magnetics*, vol. 31, no. 2, pp. 1031–1036, 1995.

[6] J. Ryoo, T.-Y. Doh, and M. Chung, "Robust disturbance obserer for the track-following control system of an optical disk drive," *Control Eng. Practice*, vol. 12, pp. 577–585, 2004.

[7] J. Yi, S. Chang, and Y. Shen, "Disturbance-observer-based hysteresis compensation for piezoelectric actuators," *IEEE/ASME Transactions on Mechatronics*, vol. 14, no. 4, pp. 456–464, 2009.

[8] B. Francis and W. Wonham, "The internal model principle of control theory," *Automatica*, vol. 12, no. 5, pp. 457–465, 1976.

[9] M. Bodson, A. Sacks, and P. Khosla, "Harmonic generation in adaptive feedforward cancellation schemes," *IEEE Transactions on Automatic Control*, vol. 39, no. 9, pp. 1939–1944, 1994.

[10] Lisa A. Sievers and Andreas H. von Flotow, "Comparison and extensions of control methods for narrow-band disturbance rejection," *IEEE Transactions on Signal Processing*, vol. 40, no. 10, pp. 2377–2391, 1992.

[11] M. Bodson and S. C. Douglas, "Adaptive algorithm for the rejection of periodic disturbances with unknown frequency," *Automatica*, vol. 33, no. 12, pp. 2213–2221, 1997.

[12] Huajin Tang, Larry Weng, Zhao Yang Dong, and Rui Yan, "Adaptive and learning control for SI engine model with uncertainties," *IEEE/ASME Transactions on Mechatronics*, vol. 14, no. 1, pp. 93–104, 2009.

[13] C. C. de Wit and L. Praly, "Adaptive eccentricity compensation," *IEEE Trans. on Control Systems Technology*, vol. 8, no. 5, pp. 157–766, 2000.

[14] K. Oldham and J. Spanier, "The fractionnal calculus," *Academic Press, New-York and London*, 1974.

[15] S. G. Samko, A. A. Kilbas, and O. I. Marichev, "Fractional integrals and derivatives: Theory and applications," *Gordon and Breach Science Publishers*, 1993.

[16] K. S. Miller and B. Ross, "An introduction to the fractional calculus and fractional differential equations," Wiley, New York, 1993.

[17] A. Oustaloup, X. Moreau, and M. Nouillant, "The CRONE suspension," *Control Engineering Practice*, vol. 4, no. 8, pp. 1101–1108, 1996.

[18] I. Podlubny, "Fractional-order systems and PID-controllers," *IEEE Trans. Automatic Control*, vol. 44, pp. 208–214, 1999.

[19] A. Oustaloup, F. Levron, B. Mathieu, and F. Nanot, "Frequency-band complex non integer differentiator: characterization and synthesis," *IEEE Transactions on Circuits and Systems*, vol. 47, pp. 25–40, 2000.

[20] D. Xue and Y. Q. Chen, "A comparative introduction of four fractional order controllers," in *Proc. of 4th IEEE World Congress on Intelligent Controllers and Automation (WCICA02)*, Shanghai, China, 2002, pp. 3228–3235.

[21] D. Valerio and J. S. da Costa, "Time-domain implementation of fractional order controllers," *IEE Proceedings - Control Theory and Applications*, vol. 152, no. 5, pp. 539–552, 2005.

[22] C. A. Monje, Y. Q. Chen, B. M. Vinagre, Dingyü Xue, and V. Feliu, *Fractional Order Systems and Controls - Fundamentals and Applications*, Springer-Verlag (Advances in Industrial Control Series), 2010.

[23] I. Podlubny, "Fractional Differential Equations," *Academic Press*, 1999.

[24] D. Chen and B. Paden, "Nonlinear adaptive torque-ripple cancellation for step motors," in *Proc. IEEE Conf. Dec. Contr.*, Honolulu, HI, 1990, pp. 3319–3324.

[25] M. Bodson, "Effect of the choice of error equation on the robustness properties of adaptive control schemes," *Int. J. Adaptive Contr. Sig. Process.*, vol. 2, no. 1, pp. 249–257, 1988.